Journal of Power Sources 199 (2012) 14–21

Contents lists available at SciVerse ScienceDirect

Journal of Power Sources

journal homepage: www.elsevier.com/locate/jpowsour

The effect of glycerol on the conductivity of Nafion-free ZrP/PTFE composite membrane electrolytes for direct hydrocarbon fuel cells

Amani Al-Othman[a,b], André Y. Tremblay[a], Wendy Pell[b], Yun Liu[b], Brant A. Peppley[c], Marten Ternan[d,*]

[a] Chemical and Biological Engineering, University of Ottawa, 161 Louis Pasteur, Ottawa, ON K1N 6N5, Canada
[b] Catalysis Centre for Research and Innovation, University of Ottawa, 30 Marie-Currie, Ottawa, ON K1N 6N5, Canada
[c] Chemical Engineering, Queens University, Dupuis Hall, Kingston, ON K7L 3N6, Canada
[d] EnPross Inc., 147 Banning Road, Ottawa, ON K2L 1C5, Canada

ARTICLE INFO

Article history:
Received 21 August 2011
Received in revised form
28 September 2011
Accepted 29 September 2011
Available online 5 October 2011

Keywords:
Zirconium phosphate
Polytetrafluoroethylene
Glycerol
Composite membranes
Proton conductivity
Hydrocarbon fuel cells

ABSTRACT

Composite membranes composed of zirconium phosphate (ZrP, a proton conductor), and porous polytetrafluoroethylene (PTFE, a mechanical support for ZrP), have been studied as electrolytes for direct hydrocarbon fuel cells that might operate at temperatures approaching 200 °C. The previous literature describes membranes formed by compressing PTFE particles and ZrP particles (conductivity = 10^{-3} S cm^{-1}). The results reported here show that adding glycerol (GLY) to a reaction mixture of $ZrOCl_2 \cdot 8H_2O$ and H_3PO_4 to form ZrP *in situ* within the pores of PTFE, produced a membrane (conductivity = 0.02–0.045 S cm^{-1}) that approached the performance of Nafion (conductivity = 0.1 S cm^{-1}). The conductivity remained unchanged when one of the membranes (conductivity = 0.02 S cm^{-1}) was processed at the inlet conditions to a direct propane fuel cell (200 °C and steam mole fraction $y_{H_2O} = 0.86$). The composite membrane, prepared with glycerol, contained ZrP spheres (100–500 nm) that were smaller than the PTFE pore diameters (1000–2000 nm). The enhanced conductivity may have been caused by a combination of proton transport on the exterior surfaces of the ZrP solid spheres, proton hopping through the bulk of the ZrP, and proton hopping via the OH groups in glycerol.

1. Introduction

High temperature operation (~200 °C) is desired in polymer electrolyte membrane (PEM) fuel cells for several reasons. It enhances reaction kinetics, improves the cell tolerance for impurities, permits the use of fuels that produce carbon monoxide, and, increases the temperature at which heat is generated, thereby allowing the recovery of useful heat.

Current PEM fuel cell technology relies on perfluorosulfonic acid (PFSA) polymer membranes (e.g. Nafion) as the proton conductive material. Nafion is the leading and the most successful electrolyte used in PEM fuel cells. Dupont developed it in the 1960s. It consists of a linear perfluorinated backbone with perfluoro side chains containing sulfonic acid groups [1].

Nafion membranes perform quite well below 90 °C under fully hydrated conditions. They also possess good chemical and mechanical stability due to the perfluorinated main chain. However, proton conductivity of this membrane is strongly dependent on its water content. Water is required to solvate the proton of the sulfonic acid groups. The substantial decrease in Nafion's proton conductivity at low hydration levels is one of the motivations toward the development of new membrane materials. For example, Nafion conductivity decreases from 0.066 to 0.00014 S cm^{-1} at 30 °C when the relative humidity (RH) decreases from 100% to 34% [2]. This is why the high temperature operation of a PEM fuel cell with Nafion is limited to temperatures below 100 °C at ambient pressure. Also Nafion starts to lose its mechanical stability above its glass transition temperature of 110 °C [3]. This is problematic because above this temperature, degradation eventually occurs. A membrane suitable for high temperature operation should have reasonable and/or high proton conductivity, good thermal and chemical stability, and low cost.

The development of high temperature membranes can be categorized into three major groups: (1) the modification of the current Nafion or PFSA membranes by the addition of hydroscopic oxides and solid proton conductors such as zirconium hydrogen phosphate $Zr(HPO_4)_2 \cdot H_2O$, (ZrP); (2) the development of sulfonated polyaromatic polymers and composite membranes, such as polyetheretherketone (PEEK) [2], and [3] the development of acid base polymer membranes such as sulphuric and phosphoric acid doped polybenzimidazole (PBI).

Considerable effort has been made to modify the existing PFSA membranes (e.g. Nafion) by the incorporation of zirconium hydrogen phosphate $Zr(HPO_4)_2 \cdot H_2O$. ZrP was one of the inorganic

* Corresponding author. Tel.: +1 613 831 8080; fax: +1 613 831 5458.
E-mail address: ternan@sympatico.ca (M. Ternan).

0378-7753/$ – see front matter © 2011 Elsevier B.V. All rights reserved.
doi:10.1016/j.jpowsour.2011.09.104

compounds suggested by Grot et al. [4]. Grot proposed that inorganic fillers, such as, the oxides and phosphates of Sn, Sb, Mo, W, Ti and Zr metals be precipitated in membranes.

Zirconium hydrogen phosphate, $Zr(HPO_4)_2{\cdot}H_2O$, belongs to the class of solid protonic conductors that has a layered structure allowing the intercalation of guest molecules. It is a highly hydroscopic insoluble solid and the interest in this compound goes back to the 1950s when it was discovered to have cation exchange properties [5–7]. Examples of composite membranes with ZrP incorporated into Nafion have been reported by: Savadogo [8] who casted a membrane using a Nafion® solution that contained zirconium (Zr^{4+}) ions, Hou et al. [9], who incorporated zirconium phosphates into Nafion 115, Bauer et al. [10] who incorporated zirconium phosphates into Nafion 1135 and 117, and Casciola et al. [11], who prepared Nafion 117–zirconium phosphate membranes.

Composite membranes using ZrP and polytetrafluoroethlyne (PTFE) have been also reported. Park et al. [12] prepared a composite membrane by mixing the particles of a PTFE emulsion with a ZrP crystalline powder, and then drying, followed by pressing. The addition of zirconium phosphate in Park's work caused the proton conductivity to increase to 2.2×10^{-3} S cm^{-1} compared to 10^{-13} S cm^{-1} for PTFE alone. Liu et al. [13] impregnated a porous polytetrafluoroethylene (PTFE) with Nafion solution to prepare Nafion/PTFE composite membranes. Jiang et al. [14] prepared Nafion–Teflon®–$Zr(HPO_4)_2$ (NTZP) composite membranes via a direct impregnation method.Research in our laboratory is directed toward the use of ZrP without using Nafion, since our target temperature is 200 °C. Our earlier work on ZrP powders [15] investigated the effect of hydration on the proton conductivity of ZrP. It showed that the water to hydrocarbon stoichiometric ratio required for direct propane fuel cells caused a substantial enhancement in ZrP proton conductivity compared to the conductivity at dry conditions. In this work ZrP particles were precipitated during an in situ reaction of $ZrOCl_2{\cdot}8H_2O$ with H_3PO_4 inside the pores of a porous PTFE membrane. The resulting composite membrane has (1) proton conducting properties, (2) thermal stability limited by PTFE (260 °C) and (3) mechanical support for the ZrP particles, provided by the PTFE. It was anticipated that this composite ZrP–PTFE membrane would be particularly suitable for direct hydrocarbon fuel cells. In this work, the effect of glycerol addition on the morphology and conductivity of the composite membrane was investigated. We were unable to find any previous experimental work specifically describing the effect of glycerol on proton conductivity in fuel cell membranes.

2. Experimental

2.1. Synthesis of a ZrP–PTFE composite membrane

There were several component materials used to make the composite membrane. The porous film was unlaminated Sterlitech PTFE (with a nominal thickness of 50 μm and a nominal pore size of 0.22 μm). $ZrOCl_2{\cdot}8H_2O$ from Sigma Aldrich was the source of the zirconium for ZrP. 85% o-phosphoric acid from Fischer Scientific was the source of phosphorous for ZrP. Ethanol (Anhydrous ethyl alcohol from Commerical Alcohols Inc.), glycerol (certified ACS, assay 99.7% from Fisher Scientific) and iso-propanol (HPLC grade, assay 99.8% from EMD Chemicals Inc.) were obtained.

The first step of the procedure was to prepare a suspension containing the $ZrOCl_2{\cdot}8H_2O$ salt having a liquid phase that would wet the surface of the porous PTFE film. Although $ZrOCl_2{\cdot}8H_2O$ dissolved readily in water, the interfacial tension between water and PTFE prevented the water from spreading on the surface of the PTFE. In contrast, both isopropanol and ethanol have lower surface tension than water; hence they wetted the PTFE surface. These alcohols were observed to penetrate through the PTFE film. In addition, fine particles of $ZrOCl_2{\cdot}8H_2O$ could be suspended in alcohol.

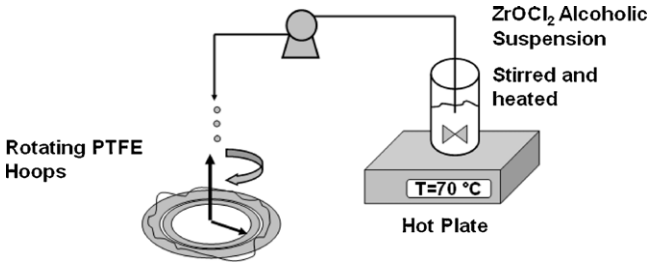

Fig. 1. Membrane synthesis set-up.

Suspensions were prepared using several methods. Two different liquid phase compositions were used: (a) 50 mL ethanol and 350 mL iso-propanol and (b) 2 mL of water plus 50 mL of ethanol and 150 mL of iso-propanol. The water dissolved much of the $ZrOCl_2{\cdot}8H_2O$. The proportion of water in the liquid was sufficiently small that the liquid mixture would wet the PTFE. As a result the total volume of the suspensions prepared with water was substantially diminished compared to the suspensions prepared without water. For some of the suspensions a small amount of glycerol (GLY) was added in order to vary the GLY/ZrP mass ratio. The suspension was placed on a stirring hot plate and vigorously mixed using a magnetic stirrer. The quantity of $ZrOCl_2{\cdot}8H_2O$ in the suspension was sufficient for the void volume of pores in the PTFE film to be filled with ZrP, $Zr(HPO_4)_2{\cdot}H_2O$. That stoichiometric amount of $ZrOCl_2{\cdot}8H_2O$ was determined from the chemical reaction [16] in Eq. (1):

$$ZrOCl_2{\cdot}8H_2O + 2H_3PO_4 \rightarrow Zr(HPO_4)_2{\cdot}H_2O + 2HCl + 8H_2O \quad (1)$$

The suspension was introduced into the pores of the PTFE film as follows: a piece of porous PTFE was weighed, and then placed between two Teflon™ hoops (concentric Teflon™ rings). The hoops were attached to a mixer shaft and rotated. As shown in Fig. 1, the stirred alcoholic suspension of $ZrOCl_2{\cdot}8H_2O$ was heated to 70 °C, pumped at a rate of 3 mL min^{-1} and, dripped onto the top side of the PTFE porous film so that it was well distributed. Periodically, dripping was stopped to allow the alcohol in the suspension to evaporate while the membrane continued to rotate. Once the membrane appeared to be dry, dripping began again. This procedure was repeated until the total amount of the alcoholic suspension had been used.

The membranes containing $ZrOCl_2{\cdot}8H_2O$ were then immersed in H_3PO_4 for 72 h. This caused the reaction in Eq. (1) to occur. Subsequently the membrane was rinsed gently with de-ionized water and isopropanol (ratio of 50:50 by volume) twice and oven dried for 24 h at 120 °C. The boiling point of glycerol is 290 °C [17]. Therefore, the majority of the glycerol was not expected to evaporate under the 120 °C maximum temperature membrane drying conditions.

A sample of the membrane prepared as described above was cut, weighed, and then further processed in a tube furnace (wet test) at 200 °C for 1.5 h with continuous H_2O injection under Argon (Ar) at an H_2O/Ar molar ratio of 6, $y_{H_2O} = 0.86$. This condition was chosen because it is the stoichiometric ratio in the direct propane fuel cell reaction where H_2O is a reactant. After processing, the membrane sample was re-weighed and placed in a sealed non-porous Teflon bag and then examined by electrochemical impedance spectroscopy (EIS).

2.2. Synthesis of a glycerol/PTFE membrane

The membranes that were composed only of PTFE and glycerol, without $ZrOCl_2{\cdot}8H_2O$, were prepared as follows. The Sterlitech

PTFE unlaminated film was cut and weighed. A specified amount of glycerol was added drop-wise while the weight was recorded on a digital balance scale. The film was then folded and cold pressed at 96.7 psi g using a Carver press, model 3856.

2.3. Investigation of the composite membrane proton conductivity

Electrochemical impedance spectroscopy (EIS) measurements were made on the various membranes. A four probe measurement method was performed using a Parstat 2273 instrument and PowerSuite 2.58, 2003 electrochemical software, over a frequency range of 1–100 kHz. The resulting impedance data were used to make Nyquist plots. The value of the real electrolyte resistance, R, was obtained from the intersection of the line on the Nyquist plot with the x-axis. After measuring the membrane thickness, d, and area, A, the proton conductivity,σ was obtained from Eq. (2) [18]:

$$\sigma = \frac{d}{R \times A} \quad (2)$$

2.4. Characterization techniques: scanning electron microscopy (SEM) and energy dispersive X-ray spectroscopy

Scanning electron microscopy (SEM) was performed using a JEOL JSM-7500F Field Emission Scanning Microscope. Prior to examination of membrane cross-sections, the membranes were immersed in liquid nitrogen and freeze–fractured. The freeze-fractured samples were further studied using the COMPO (composition analysis) feature in SEM, i.e., the use of back scattered electrons in order to detect the contrast between areas of different compositions (atomic numbers) at the membrane cross section. Energy-dispersive X-ray spectroscopy (EDS) was used to identify the elemental composition of some samples.

3. Experimental results

3.1. Membrane morphology studies

The composite membranes prepared in this study have two solid phase components, zirconium phosphate (ZrP) and a porous polytetrafluoroethylene (PTFE) film, plus in some cases a liquid phase component, glycerol (GLY). Previously we investigated ZrP powder without the PTFE film [15]. A scanning electron micrograph (SEM) of the PTFE film used in the composite membranes is shown in Fig. 2(a) in its as received condition. The spaces between the strands of PTFE form pores that appear to be oblong in shape with a typical narrow dimension near 1 μm and a typical long dimension near 2 μm. These dimensions are somewhat different than the 0.22 μm pore size provided by the manufacturer. The 0.22 μm pore size is the absolute pore size value that was determined by the manufacturer using the bubble point test with isopropanol.

The SEM image in Fig. 2(b) shows a ZrP composite membrane after the PTFE pores had been filled with ZrP using a preparation method that did not use glycerol. The surface is composed of flakes of zirconium phosphate material (ZrP) that cover the PTFE surface. A typical flake size is greater than 1 μm. Conductivity, in the order of 10^{-5} S cm^{-1} was reported for this membrane.

The top view of a ZrP–PTFE composite membrane prepared using a GLY/ZrP mass ratio, $MR_{GLY/ZrP}$, of 0.4 is shown in Fig. 3. Fig. 3(a) and (b) is for the same film but at different magnifications, 1900 for (a) and 5000 in (b). The comparison between Figs. 2 and 3 reveals a difference in morphology. The presence of glycerol has changed the ZrP particles morphology from the flakes larger than 1 μm in Fig. 2(b) into nearly spherical particles in the range of 100–500 nm that have formed aggregates in some regions. In addition, it is apparent that the spherical particles in Fig. 3(b) are definitely smaller than the pore dimensions in Fig. 2(a).

One possible explanation for the spherical shape of the particles is that the glycerol molecules, $HOCH_2–CHOH–CH_2OH$, might have occupied positions near the $ZrOCl_2{\cdot}8H_2O$ solid. Specifically the OH groups might have been adjacent to the $ZrOCl_2{\cdot}8H_2O$ solid and the CH or CH_2 groups might have been adjacent to the PTFE. Such positioning would be consistent with the values of solubility parameters that can be used to assess the compatibility of materials. One common use of solubility parameters is to describe miscibility of two liquid phase components (like dissolves like). In this case PTFE has a solubility parameter of 14 MPa$^{1/2}$. Examples of solubility parameters of alkanes are pentane = 14.4 MPa$^{1/2}$ and hexane = 14.9 MPa$^{1/2}$. The solubility parameters for the CH and CH_2 groups (alkane structures) in glycerol might be similar to the solubility parameter for PTFE. Similarly $ZrOCl_2{\cdot}8H_2O$ has many OH groups that would be compatible with the OH groups in glycerol. Specifically, the solubility parameter for water is 47.8 MPa$^{1/2}$ and

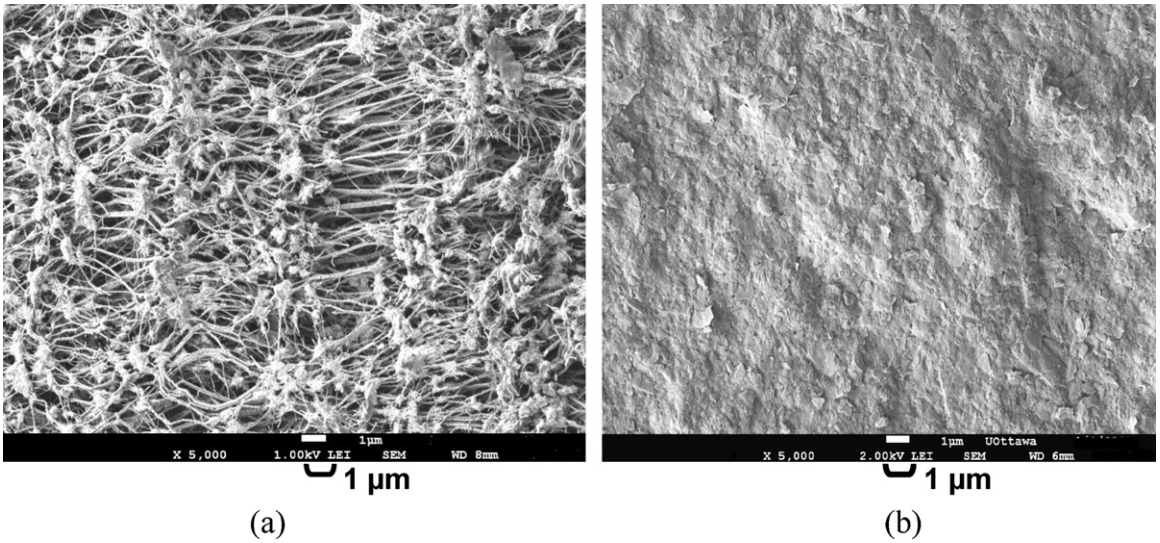

Fig. 2. Scanning electron microscopy (SEM) images for; (a) top view of the Sterlitech PTFE (Teflon®) film as received and (b) top view of a ZrP–PTFE composite membrane prepared without the use of glycerol.

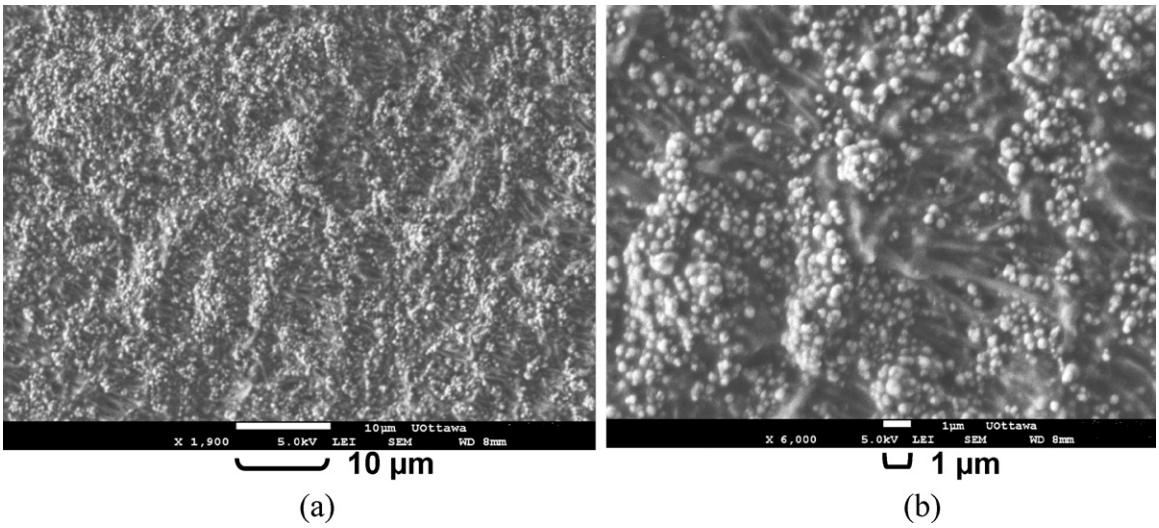

Fig. 3. Scanning electron microscopy (SEM) images for: top view of a ZrP–PTFE membrane prepared with a GLY/ZrP mass ratio of 0.4, having magnifications of (a) 1900 and (b) 5000.

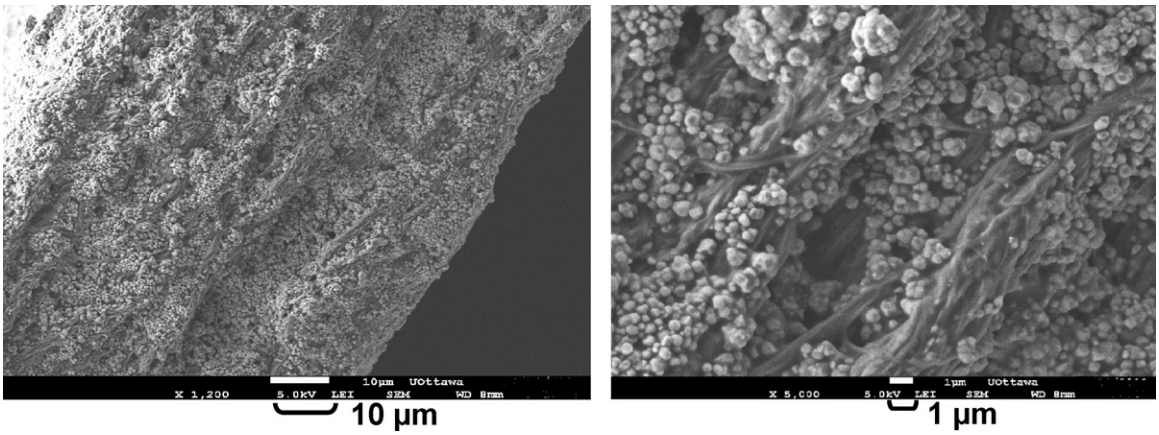

Fig. 4. SEM image for a cross sectional view of ZrP–PTFE membrane prepared with a GLY/ZrP mass ratio of 0.4 at different magnifications.

the value for glycerol (OH groups plus CH groups) is 36.2 $MPa^{1/2}$. These numbers suggest that glycerol would be a suitable molecule to be located at the interface between a hydrophobic region, PTFE, and a hydrophilic region $Zr(HPO_4)_2{\cdot}H_2O$. Nafion, one of the best fuel cell membranes, also has hydrophobic and hydrophilic regions.

Furthermore, the small spherical shape of the ZrP particles/aggregates seen in the SEM images might have resulted from

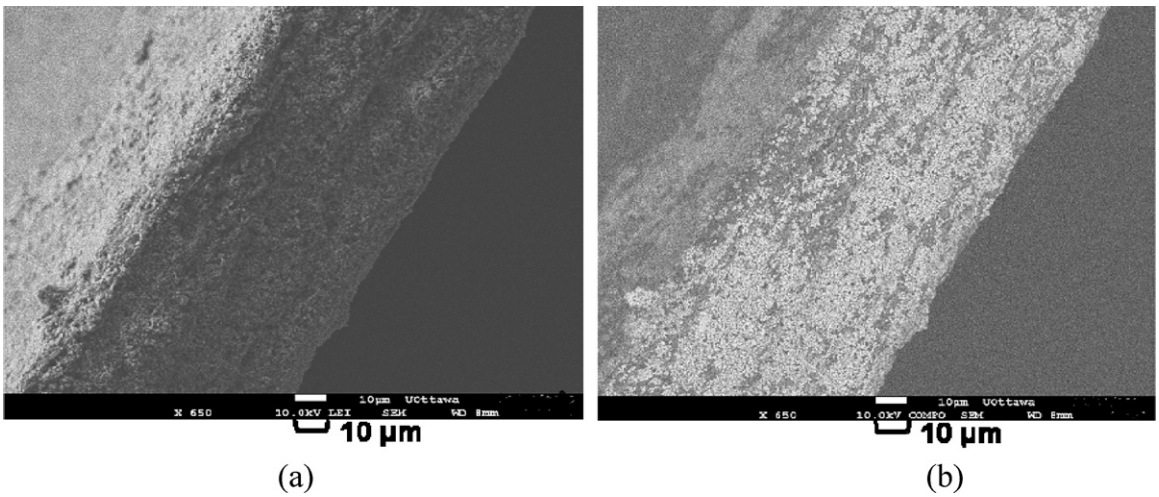

Fig. 5. SEM image for; (a) cross sectional view of ZrP–PTFE membrane prepared with a GLY/ZrP mass ratio of 0.4 and (b) same image but using the composition analysis (COMPO feature) in SEM.

the presence of glycerol that has a high surface tension, combined with successive wetting and drying cycles inside the confined PTFE hydrophobic pores.

A cross-sectional view of the same ZrP–PTFE composite membrane shown in Fig. 3 (top view) is shown after freeze-fracturing in Fig. 4 at two magnifications. At the higher magnification several features of the composite membrane morphology can be seen: individual ZrP particles, agglomerates of ZrP particles, some strands of the PTFE polymer, and some void spaces. The void spaces are undesirable since if they were connected, they would provide a path for species to cross over the membrane from one electrode to the other. The SEM image of the membrane cross-section in Fig. 4 at the higher magnification confirms the individual particle size range of 100–500 nm.

A cross sectional view after freeze-fracturing of a different composite membrane, having a GLY/ZrP mass ratio, $MR_{GLY/ZrP}$, of 0.4 is shown in Fig. 5a. The composition of the cross-section was measured by the COMPO feature in SEM, which reveals a contrast based on the atomic number of each component, i.e., ZrP appears in a whiter shade. The results are shown in Fig. 5(b). At this scale of

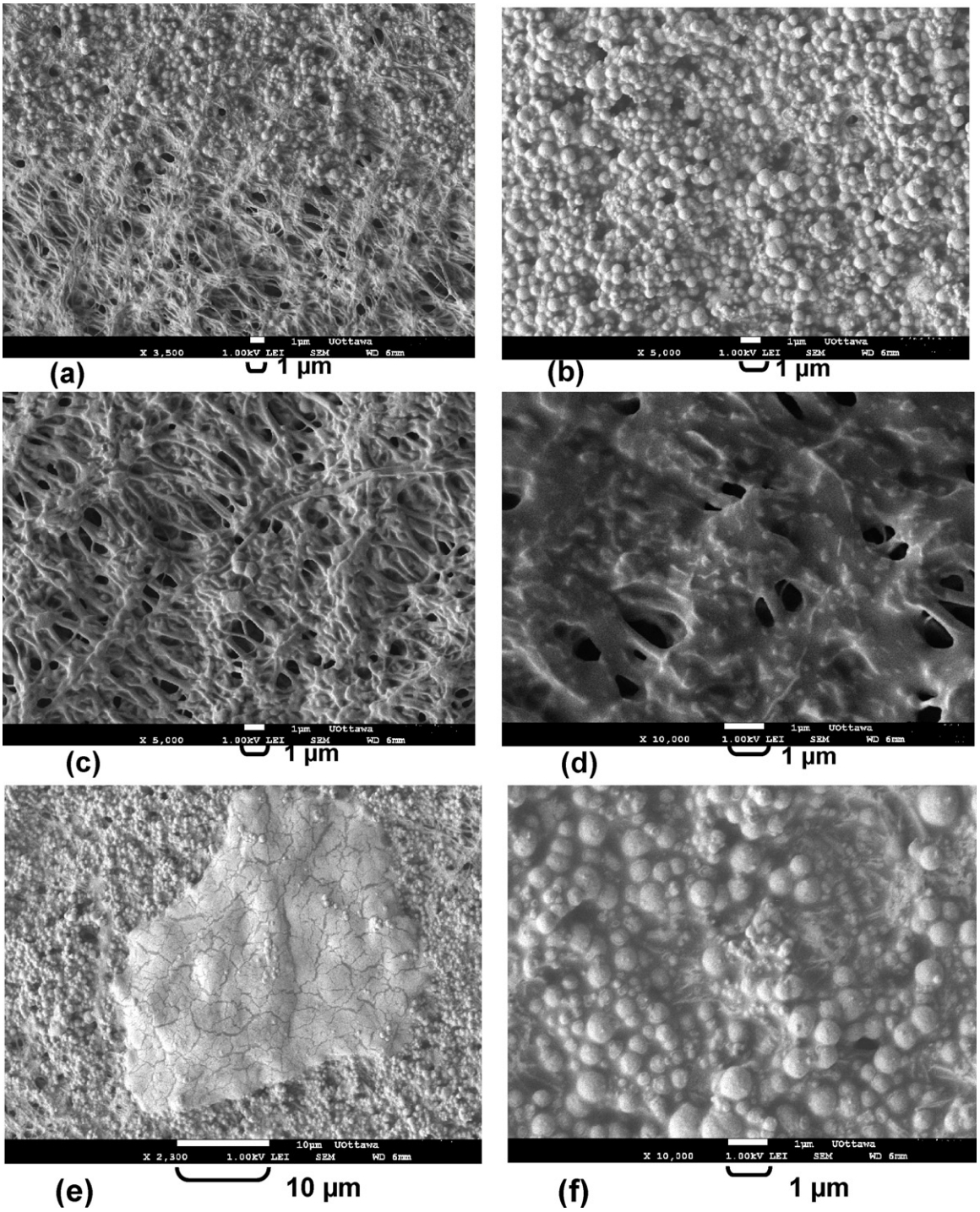

Fig. 6. A top view SEM image of a ZrP–PTFE composite membrane prepared with a GLY/ZrP mass ratio of 0.8. (a) Two distinct regions in the same range, an upper region of ZrP particles and a lower region of empty pores, (b) and (f) ZrP particles at greater magnifications, (e) a large agglomerate of ZrP on top of the ZrP particles, (c) and (d) empty pores at greater magnifications showing the presence of a fluid-like material (glycerol) adhering to the strands of PTFE.

observation it appears that the ZrP particles were deposited almost uniformly across the thickness of the composite membrane, indicating that the pores were filled with ZrP.

SEM images for a ZrP–PTFE composite membrane with a GLY/ZrP mass ratio, $MR_{GLY/ZrP}$, of 0.8 are shown in Fig. 6. Two different regions are apparent in Fig. 6(a). The dominant feature in the upper region is the ZrP particles, indicating that the pores in that region have been filled with ZrP particles. The particle diameters in Fig. 6(b) and (f) appear to be distributed over a larger range, 100–1000 nm, than those shown in Figs. 3 and 4. In Fig. 6(e) a large agglomerate of ZrP is seen to be on top of ZrP particles. The lower region in Fig. 6(a) appears to consist of empty pores. However, at higher magnifications, Fig. 6(c) and (d) suggests that the pores are partially filled with a fluid like material (glycerol) in which isolated ZrP particles with diameters slightly greater than 100 nm appear to be embedded.

The observations of (a) empty pores within the membrane and (b) ZrP plates on the exterior of the membrane are consistent with the preparation method. At a GLY/ZrP mass ratio of 0.8, the volume of glycerol plus $ZrOCl_2{\cdot}8H_2O$ in the suspension exceeds the pore volume of the PTFE. Therefore during the dripping step of the membrane synthesis there will be a point at which all the pores have been filled with glycerol plus $ZrOCl_2{\cdot}8H_2O$, but not all of the $ZrOCl_2{\cdot}8H_2O$ necessary to fill the pores (Fig. 6(c)) will have been dripped onto the PTFE. As the dripping step continues the additional glycerol and at least some of the additional $ZrOCl_2{\cdot}8H_2O$ [and as a result eventually some of the ZrP] will be located on the exterior of the PTFE, Fig. 6(f). The presence of glycerol inside the pores without the corresponding quantity of $ZrOCl_2{\cdot}8H_2O$ would support the suggestion that there would be some pores that do not contain ZrP. In addition the deposition of glycerol plus $ZrOCl_2{\cdot}8H_2O$ on the membrane exterior after all the pores had been filled with glycerol would suggest that ZrP deposits (flakes) would be formed on the membrane exterior.

EDS measurements (not shown here) were performed on the agglomerated region that appeared in Fig. 6(e). The results for the agglomerate were compared with other EDS analyses for $ZrOCl_2{\cdot}8H_2O$ and for ZrP powder. The composition of the agglomerated region resembled that of ZrP with a minor shift in some peaks, plus large oxygen peaks. High oxygen content was attributed to the presence of glycerol. This suggested that the agglomerated region in Fig. 6(e) is ZrP material associated with glycerol.

3.2. Effect of glycerol on conductivity in films of PTFE

The conductivity of the porous PTFE film (Sterlitech unlaminated film) used in these composite membranes was tested by EIS, as received and with no additives. An erratic or irregular pattern was apparent. Such a pattern might be expected for a material that does not posses proton conducting properties. Conductivities for PTFE as low as 10^{-13} S cm^{-1} have been reported in literature [12].

Different amounts of glycerol were added to a set of porous Sterlitech PTFE films. Their impedance plots are shown in Fig. 7 as a function of the GLY/PTFE mass ratio $(MR)_{GLY/PTFE}$. The presence of glycerol caused the PTFE film to change from being an insulator material to being a conductor. Specifically, the resistance of the PTFE film decreased as its glycerol content increased. Overall, glycerol in the PTFE film caused the conductivity to increase by several orders of magnitude, from 10^{-13} S cm^{-1} to 10^{-4} S cm^{-1}. In the Nyquist plot, the imaginary component of the impedance is a linear function of the real component of the impedance. That linear relationship is typically associated with proton conduction being related to a diffusion phenomenon that results from a gradient in the concentration.

The resistances obtained in Fig. 7 are shown in Table 1. The conductivities were calculated from the resistances using Eq. (2), and

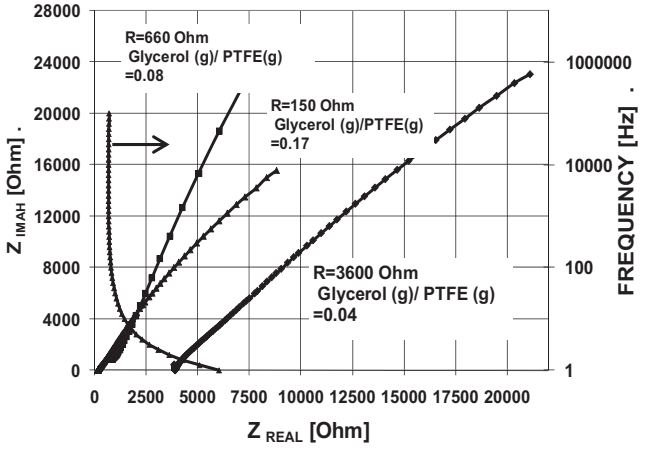

Fig. 7. Electrochemical impedance spectroscopy pattern for a porous Sterlitech PTFE films containing specified GLY/PTFE mass ratios.

Table 1
Resistances of PTFE films containing glycerol.

Mass ratio [GLY/PTFE] $MR_{GLY/PTFE}$	Resistance [Ohms]	Conductivity [S cm^{-1}]
0.04	3600	6.49×10^{-6}
0.08	660	3.50×10^{-5}
0.17	150	1.56×10^{-4}

are also shown in Table 1. It is seen that there is a linear relationship between the GLY/PTFE ratio and the conductivity.

EIS measurements were also made on the composite membranes that had been prepared by filling the pores of the PTFE film with solid particles of zirconium phosphate. A Nyquist plot obtained by EIS for a ZrP–PTFE composite membrane that did not contain any glycerol is shown in Fig. 8. The semi-circular shape on the left-hand (high frequency) side of the Nyquist plot in Fig. 8 is typically associated with a combination of (a) a double layer and (b) charge transfer reaction kinetics, resulting from a gradient in the electrical potential. The linear portion at the low frequency end of Fig. 8 is typically associated with diffusion resulting from a concentration gradient. It is similar in shape to those reported in the literature for crystalline ZrP [19] but different than some of our previous results for amorphous ZrP [15]. Its resistance ($R = 1000\ \Omega$) and conductivity (1.7×10^{-5} S cm^{-1}) were of the same order of magnitude as the values for PTFE films that contained glycerol. That observation suggests that the addition of ZrP to PTFE has an

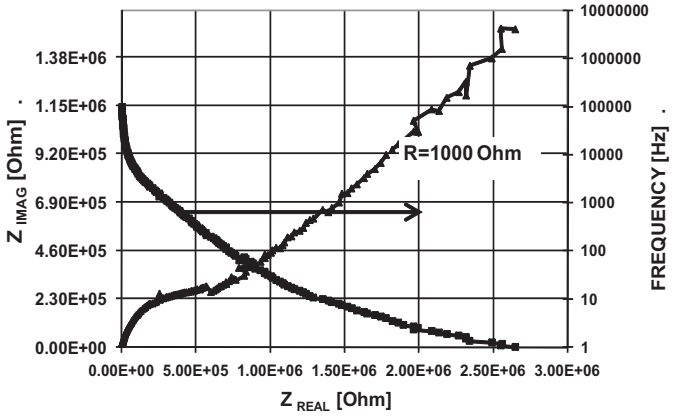

Fig. 8. Electrochemical impedance spectroscopy pattern for a ZrP–PTFE composite membrane that did not contain glycerol.

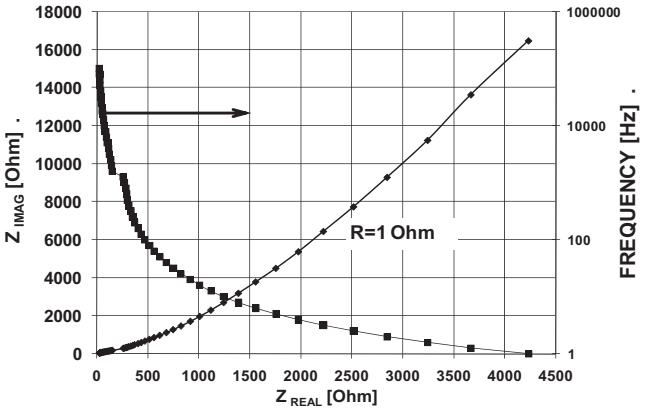

Fig. 9. Electrochemical impedance spectroscopy pattern for a ZrP–PTFE composite membrane having a glycerol/ZrP mass ratio of 0.4.

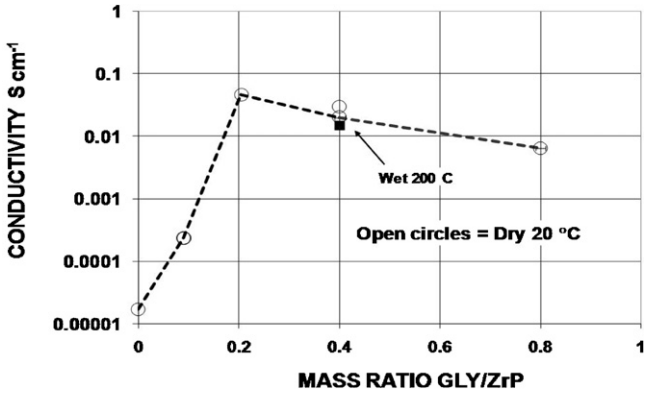

Fig. 11. Change of proton conductivity (σ) S cm^{-1} with glycerol/ZrP mass ratio in the composite membrane.

influence on the magnitude of the conductivity that is somewhat similar to the addition of glycerol.

A Nyquist plot is shown in Fig. 9 for a ZrP–PTFE composite membrane to which glycerol had been added. Its glycerol to ZrP mass ratio, $MR_{GLY/ZrP}$ was 0.4. The resistance of the glycerol containing composite membrane in Fig. 9 was orders of magnitude less than that of the glycerol-free composite membrane in Fig. 8. While the conductivities of the two component materials, 6.9×10^{-5} to 1.5×10^{-4} S cm^{-1} for the GLY/PTFE membrane in Fig. 7, and 1.7×10^{-5} S cm^{-1} for the ZrP/PTFE membrane in Fig. 8, were much greater than PTFE alone, the combination of the three components, in Fig. 9, had a conductivity, 2×10^{-2} S cm^{-1}, that was vastly superior to either of the two component materials. The shape of the Nyquist plot in Fig. 9 is indicative of diffusion.

A Nyquist plot for a ZrP composite membrane having an $MR_{GLY/ZrP}$ of 0.8 is shown in Fig. 10. In general its shape was similar to that in Fig. 9. However, its resistance, 3 Ohms, was slightly larger and its conductivity, 6.5×10^{-3} S cm^{-1}, was slightly smaller than the corresponding values derived from Fig. 9. The poorer performance with an $MR_{GLY/ZrP}$ value of 0.8 is consistent with the morphology seen in Fig. 6, where some of the pores did not contain ZrP particles and the external membrane surface contained comparatively large ZrP agglomerates.

The conductivity results for the GLY/ZrP/PTFE composite membranes are shown in Fig. 11 as a function of the GLY/ZrP mass ratio, $MR_{GLY/ZrP}$. The proton conductivity increased by several orders of magnitude when glycerol was introduced to the ZrP/PTFE composite membranes. The proton conductivity reached a maximum value (0.02–0.045 S cm^{-1}) when the GLY/ZrP mass ratio was in the region of 0.2–0.4. It is also evident from Fig. 11 that the proton

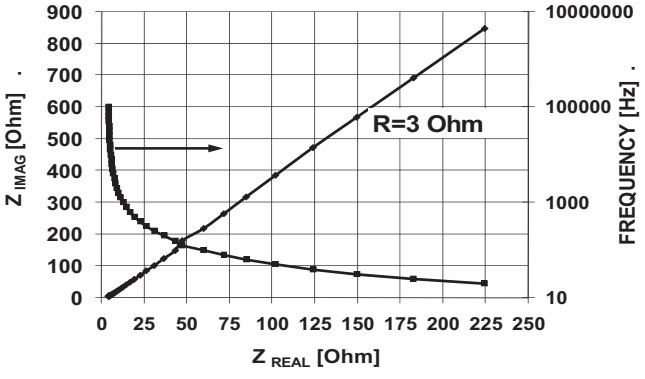

Fig. 10. Electrochemical impedance spectroscopy pattern for a ZrP–PTFE composite membrane having a glycerol/ZrP mass ratio of 0.8.

conductivity decreased by almost an order of magnitude when the $MR_{GLY/ZrP}$ was increased to 0.8. This result is consistent with what was presented earlier by the SEM images showing that larger spherical particles were formed at this $MR_{GLY/ZrP}$ ratio, i.e., a decrease in the total surface area of ZrP particles leads to a decrease in the proton conductivity. Furthermore, the non-uniform distribution of ZrP and the appearance of two distinctive regions of ZrP and glycerol (referring to Fig. 6(a) and (e) might have contributed to the decrease in proton conductivity.

Proton hopping is generally considered to be the mechanism that is responsible for proton conductivity. For example, proton hopping in water has been extensively reviewed [20]. Similarly, protons could be expected to hop between the oxygen atoms in the OH groups in glycerol, $HOCH_2–CHOH–CH_2OH$. That might be an explanation for the conductivity observed in GLY/PTFE membranes. In ZrP, each zirconium atom is associated with a $Zr(HPO_4)_2{\cdot}H_2O$ structure that has two OH groups and one H_2O molecule. Hopping between the oxygen atoms in the OH groups and the water of hydration within a $Zr(HPO_4)_2{\cdot}H_2O$ structure molecule might be expected.

Proton conductivity on the external surfaces of ZrP particles has also been suggested as a phenomenon. Alberti et al. [21,22] showed that the conductance of ZrP decreased with the increase in the degree of crystallinity and that although the fraction of the surface covered with protons is small, their mobility is 10^4 greater than the protons in the bulk. Thus, greater external ZrP surface area, results in greater proton conductivity.

The conductivity results obtained in this work have been compared with some literature values in Table 2. PTFE is an insulator. In contrast the conductivity of ZrP particles is orders of magnitude greater than for PTFE. When the void volume of porous PTFE was filled with glycerol, the conductivity was as good as or better than that of ZrP particles. When a dry ZrP/PTFE membrane was composed of a combination of a porous PTFE film plus flakes of ZrP the conductivity was comparable to that of dry ZrP particles. However when the ZrP/PTFE membrane was composed of a combination of PTFE particles and ZrP particles compressed together, there was an order of magnitude increase in the conductivity compared to the combination of porous PTFE and ZrP flakes. Finally when ZrP was formed *in situ* within the pores of a porous PTFE in the presence of glycerol, the conductivity increased by two orders of magnitude. The conductivity of the GLY/ZrP/PTFE composite membrane approached 40% of the value for Nafion. Furthermore, that value was maintained when the temperature was increased from 20 to 200 °C provided the steam to feedstock ratio was typical of that required for a direct propane fuel cell.

The inclusion of glycerol in the GLY/ZrP/PTFE membrane made two differences. The morphology of the ZrP changed from flakes to

Table 2
Summary of conductivity results.

Material	Proton Conductivity [Scm^{-1}]	
	Literature values	This work
PTFE [12] ZrP (particles)	10^{-13}	
Crystallites – dry [23,24]	10^{-6}–10^{-5}	
Amorphous – dry [15]	10^{-5}	
Amorphous – wet [15]	10^{-4}	
GLY/PTFE (porous film)		$0.7–1.5 \times 10^{-4}$
ZrP(particles) – PTFE (particles) – dry [12]	10^{-4}–10^{-3}	
ZrP(flakes) – PTFE (porous film) – dry [15]	10^{-5}	1.7×10^{-5}
ZrP(flakes) – PTFE (porous film) – wet ($y_{H_2O} = 0.86$ at 200 °C) [15]	10^{-4}	
GLY – ZrP(spheres) – PTFE(porous film) – dry		0.02–0.045
GLY – ZrP(spheres) – PTFE(porous film) – wet ($y_{H_2O} = 0.86$ at 200 °C)		0.015
Nafion – 20 °C and 95% Relative humidity [25]	0.12	
–120 °C and 90% Relative humidity [25]	0.013	

small spheres. Also the surfaces of the solid ZrP spheres were in contact with glycerol. It is possible that the enhancement in conductivity in the GLY/ZrP/PTFE membranes may have been caused by proton transport at the interface between the small solid ZrP spheres and their glycerol coating. In addition to two bulk phenomena, proton transport though ZrP and proton transport through glycerol, surface phenomena may have also contributed to the conductivity. Presumably two surface phenomena, proton transport on solid ZrP surfaces and proton hopping via the OH groups in glycerol, may have been operating simultaneously. Because the PTFE pores contained a large number of small spheres, together they would have a large surface area. The combination of the two proton surface transport mechanisms plus the large interfacial area may help to explain the two order of magnitude improvement in conductivity. Furthermore, the high surface tension of glycerol and the successive wetting and drying cycles inside the hydrophobic pores have favoured the formation of small aggregates of $ZrOCl_2$. The presence of glycerol has prevented these aggregates from coalescing; hence, the formation of nano-scale particles within the confined environment existing in the PTFE pores. These particles were relatively spherical in shape resulting in a high total surface area and a highly conducting membrane.

4. Conclusions

Glycerol was found to enhance the proton conductivity when added to both a porous PTFE film and a ZrP/PTFE composite membrane. Small spheres of ZrP (100–500 nm) were observed in the GLY/ZrP/PTFE composite membrane. The enhanced conductivity may have been caused by a combination of proton transport on the increased surface area on the exterior of the small ZrP spheres plus proton hopping using both the OH groups in glycerol and the ZrP bulk. The conductivity of GLY/ZrP/PTFE composite membranes at 20 °C approached 40% of the conductivity of a Nafion membrane. This proton conductivity was maintained when the membrane was processed at 200 °C in the presence of a steam partial pressure typical of a direct propane fuel cell. For fuel cell operations above the boiling point of water, these membranes could be promising alternatives to Nafion membranes.

Acknowledgments

The authors are grateful for the financial support from the Canadian federal government's Natural Sciences and Engineering Research Council and from the Ontario provincial government's Ministry of Research and Innovation (Ontario Fuel Cell Research and Innovation Network). The authors wish to also thank Dr. Takeshi Matsuura for his assistance in providing some literature references.

References

[1] P.J. James, J.A. Elliot, T.J. McMaster, J.M. Newton, A.M.S. Elliot, S. Hanna, M. Miles, J. Mater. Sci. 35 (2000) 5111.
[2] J.L. Zhang, Z. Xie, J. Zhang, Y. Tang, C. Song, T. Navessin, Z. Shi, D. Song, H. Wang, D. Wilkinson, Z. Liu, S. Holdcroft, J. Power Sources 160 (2006) 872.
[3] C. Yang, S. Srinivasan, A. Bocarsly, S. Tulyani, J.B. Benziger, J. Membr. Sci. 237 (2004) 145.
[4] W.G. Grot, G. Rajendran, US Patent 5,919,583, (1999).
[5] C.B. Amphelett, L.A. McDonald, M.J. Redman, J. Inorg. Nucl. Chem. 6 (1958) 220.
[6] A. Clearfield, J.A. Stynes, J. Inorg. Nucl. Chem. 26 (1964) 117.
[7] R.P. Hamlen, J. Electrochem. Soc. 109 (1962) 746.
[8] O. Savadogo, J. Power Sources 127 (2004) 135.
[9] H. Hou, G. Sun, Z. Wu, W. Jin, Q. Xin, Int. J. Hydrogen Energy 33 (2008) 3402.
[10] F. Bauer, M. Willert-Porada, Fuel Cells 6 (2006) 261.
[11] M. Casciola, D. Capitani, A. Comite, A. Donnadio, V. Frittella, M. Pica, M. Sganappa, A. Varzi, Fuel Cells 8 (2008) 217.
[12] Y. Park, K. Jae-Dong, M. Nagai, J. Mater. Sci. Lett. 19 (2000) 1735.
[13] F. Liu, B. Yi, D. Xing, J. Yu, H. Zhang, J. Membr. Sci. 212 (2003) 213.
[14] R. Jiang, H.R. Kunz, J. Fenton, Electrochim. Acta 51 (2006) 5596.
[15] A. Al-Othman, A.Y. Tremblay, W. Pell, S. Letaief, T.J. Burchell, B.A. Peppley, M. Ternan, J. Power Sources 195 (2010) 2520.
[16] H.L. Lin, S.H. Yeh, T.L. Yu, L.C. Chen, J. Polym. Res. 16 (2009) 519.
[17] M.C. Burshe, S.B. Sawant, V.G. Pangarkar, J. Am. Oil Chem. Soc. 76 (1999) 209.
[18] Y.J. Wang, Y. Pan, L. Chen, Mater. Chem. Phys. 92 (2005) 354.
[19] D. Bianchi, M. Casciola, Solid State Ionics 17 (1985) 7.
[20] E. Gileadi, E. Kirowa-Eisner, Electrochim. Acta 51 (2006) 6003.
[21] G. Alberti, E. Torracca, J. Inorg. Nucl. Chem. 30 (1968) 1093.
[22] G. Alberti, M. Casciola, U. Costantino, G. Levi, G. Ricciardi, J. Inorg, Nucl. Chem. 40 (1978) 533.
[23] H. Patel, U. Chudasam, J. Chem. Sci. 119 (2007) 35.
[24] A. Clearfield, Annu. Rev. Mater. Sci. 14 (1984) 205.
[25] M. Casciola, G. Alberti, M. Sganappa, R. Narducci, J. Power Sources 162 (2006) 141.